///VSP///

Journal of Biomaterials Science 21 (2010) 205–223

Journal of BIOMATERIALS SCIENCE
brill.nl/jbs

Gene Delivery Efficacy of Polyethyleneimine-Introduced Chitosan Shell/Poly(methyl Methacrylate) Core Nanoparticles for Rat Mesenchymal Stem Cells

Nuttaporn Pimpha [a], **Panya Sunintaboon** [b], **Supharat Inphonlek** [b] **and Yasuhiko Tabata** [c,*]

[a] National Nanotechnology Center, Thailand Science Park, Paholyothin Rd., Pathumthani, 12120, Thailand

[b] Department of Chemistry, Faculty of Science, Mahidol University, Bangkok, 10400, Thailand

[c] Department of Biomaterials, Field of Tissue Engineering, Institute for Frontier Medical Sciences, Kyoto University, 53 Kawara-cho Shogoin, Sakyo-ku, Kyoto 606-8507, Japan

Received 15 October 2008; accepted 19 January 2009

Abstract

This work investigated polyethyleneimine (PEI)-introduced chitosan (CS) (CS/PEI) nanoparticles as non-viral carrier of plasmid DNA for rat mesenchymal stem cells (MSCs). The CS/PEI nanoparticles were prepared by the emulsifier-free emulsion polymerization of methyl methacrylate monomer induced by a small amount of *t*-butyl hydroperxide in the presence of different concentrations of PEI mixed with CS. The resulting nanoparticles were characterized by their surface properties and buffering capacity. *In vitro* gene transfection was also evaluated. The introduction of PEI affected the surface charge, dispersing stability and buffering capacity of the nanoparticles. The CS/PEI nanoparticles formed a complex upon mixing with a plasmid DNA of luciferase. The complex enhanced the level of gene transfection and prolonged the time period of expression for MSCs, compared with those of plasmid DNA–original CS and PEI nanoparticles. Cytotoxicity of CS/PEI complexes with plasmid DNA was significantly low, depending on the amount of PEI introduced. It is concluded that the CS/PEI nanoparticle was a promising carrier for gene delivery of MSCs.

© Koninklijke Brill NV, Leiden, 2010

Keywords

Nanoparticles, chitosan, polyethyleneimine, mesenchymal stem cells, non-viral carrier

* To whom correspondence should be addressed. Tel.: (81-75) 751-4121; Fax: (81-75) 751-4646; e-mail: yasuhiko@frontier.kyoto-u.ac.jp

© Koninklijke Brill NV, Leiden, 2010

DOI:10.1163/156856209X415503

1. Introduction

Mesenchymal stem cells (MSCs) have the potential to induce the regeneration of mesenchymal tissues, such as bone, cartilage, muscle, ligament, tendon, adipose and marrow stroma tissues. The cells can be differentiated effectively into the adipocytic, chondrocytic, or osteocytic lineages [1–3]. Based on the biological aspects, MSC-based therapy is one of the promising approaches to achieve the regeneration and repairing of tissues [4–11]. It is expected for more effective cell therapy to use MSC genetically modified for the functional activation. For example, Meinel *et al.* studied the cell therapy of human MSC genetically engineered with adenovirus, containing a human BMP-2 gene in the combination with silk scaffold [12]. Ahn *et al.* examined PEI as a carrier of gene transfection for human adipose tissue-derived stem cells [13]. Uludag and co-workers reported the effectiveness of an amphiphilic poly(L-lysine)-palmitic acid in the plasmid DNA carrier for bone marrow stromal cells [14]. Moreover, Hosseinkami *et al.* have prepared cationized polysaccharides for a non-viral gene carrier to enhance the DNA expression of MSC [15] and demonstrated the therapeutic efficacy in acute cardiac infarction [16].

To effectively transfect cells, various viral and non-viral carriers have been extensively investigated. Compared with the viral carrier, although a non-viral one is less effective in term of gene transfection, it has superior safety profiles and low immunogenicity. Therefore, it a great challenge to develop effective non-viral carriers for successful gene therapy.

Among the non-viral carriers, cationic polymers have attracted great attention, since they can complex with plasmid DNA through the electrostatic interaction. Moreover, their properties can easily be modified by changing the constituents of monomer, controlling the polymerization conditions, or chemically introducing functional groups to the polymers. In addition, the composition can be easily manipulated by the conjugation with a targeting ligand or intracellular trafficking enhancer [17]. Polyethyleneimine (PEI) is one of the most promising non-viral carriers because it shows a proton sponge effect [18]. However, for the clinical application, PEI has some problems to be resolved, such as its biodegradability and toxicity. Consider on biodegradability and toxicity, much attention has been given to chitosan (CS), since it possesses interesting properties such as biocompatibility, biodegradability, film forming ability, gelation characteristics, and bioadhesion. Moreover, because of its polycationic nature, CS has been extensively investigated for carrier and delivery systems of negatively charged agents. CS is also a good candidate for a plasmid DNA carrier that has been extensively investigated, but the transfection efficiency is still low. It has been reported that the low ability of gene transfection is due to the instability of CS–DNA complexes, which results in the aggregation at the outside of cell membrane, and, consequently, poor cellular internalization [19]. Moreover, no buffering effect necessary for the endosomal escape of complex is another disadvantage [20–22]. It is practically necessary to develop a new non-viral carrier of gene transfection by combining the material advantage of PEI and CS.

In this study, CS/PEI nanoparticles were prepared by an emulsifier-free emulsion polymerization in the presence of PEI and chitosan. The PEI/CS weight ratio in preparation was changed systematically to evaluate the effect on particle size, surface charge and buffering capacity. Following the incubation with MSCs, the level of gene expression and the expression period were evaluated and compared with those of CS and PEI nanoparticles.

2. Materials and Methods

2.1. Materials

CS was purchased from Seafresh Chitosan Lab. (Thailand). The degree of deacetylation was *ca.* 85%, and the weight-average molecular weight of CS was *ca.* 45×10^3, determined by a viscometric method. Branch polyethyleneimine (PEI; molecular weight 750×10^3) was purchased from Aldrich. Methyl methacrylate (MMA) and *t*-butyl hydroperoxide (TBHP) were purchased from Fluka. TBHP was used as obtained. MMA was purified to remove inhibitors using a column packed with alumina adsorbent. PEI was diluted with deionized water to 10 wt% and carefully adjusted with HCl until the pH 7. Deionized (DI) and autoclaved water were sterilized and used throughout the study. All other chemicals were commercially available and of analytical grade.

2.2. Methods

2.2.1. Preparation of PEI-Introduced Chitosan Nanoparticles

The emulsifier-free emulsion polymerization was carried out by the aid of the amine/TBHP initiating system as illustrated in Fig. 1. Both PEI and chitosan have plenty of amine groups on their backbones capable of forming initiating system with TBHP. The resulting radicals on the nitrogen atoms of amines were then propagated with vinyl monomers. By using this polymerization method, core–shell nanoparticles can be formed with PEI and chitosan as a shell and vinyl polymer as a core [23]. The synthetic procedure was briefly described as follows: The polymerization was conducted in a 100-ml water-jacketed glass reactor equipped with a reflux condenser, nitrogen inlet, thermostat water bath, and magnetic stirrer. A total reaction volume of 50 ml was generally used. CS (0.5 g), predissolved in 1% acetic acid, and deionized water were mixed with PEI (10 wt%, pH 7) solution. The weight ratio of CS to PEI was varied (0.5:0, 0.5:0.1, 0.5:0.3, 0.5:0.5 and 0:0.5). The mixture was purged with nitrogen gas for 30 min. Water was pumped through the jacketed reactor from a thermostat water bath, which was controlled at 80 ± 1°C. The MMA monomer (1 g) was added, followed by an addition of TBHP aqueous solution (1 g, 5×10^{-3} M) to initiate polymerization. Then, the polymerization was continued for 2 h under nitrogen atmosphere. The homopolymer and unreacted monomer were removed by Soxhlet extraction.

2.2.2. Determination of Monomer Conversion and Solid Content

The monomer conversion and solid content were determined gravimetrically. About

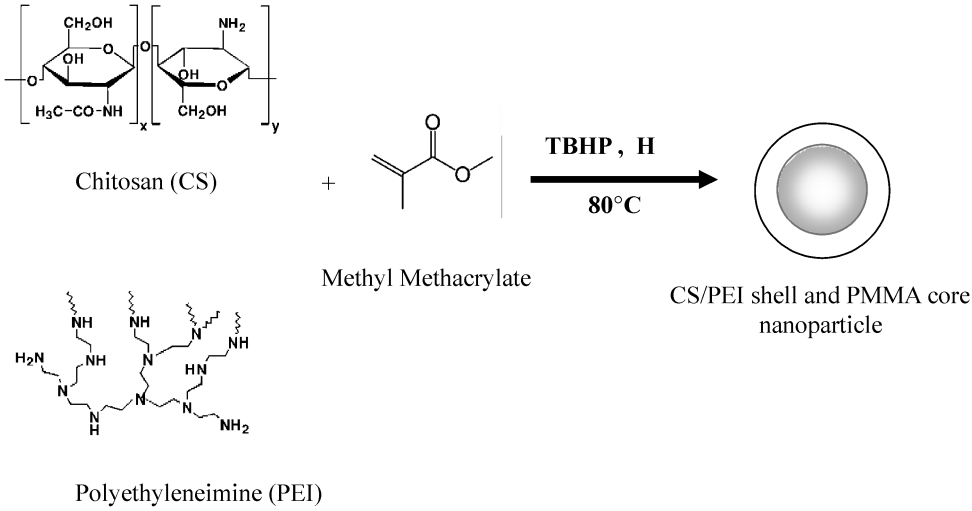

Figure 1. Scheme of emulsifier-free emulsion polymerization in the presence of different concentrations of PEI mixed with CS under N_2 atmosphere at 80°C for 2 h for CS/PEI nanoparticles preparation.

2 g nanoparticle latex prepared was taken into a pre-weighed aluminum pan. After complete evaporation in a fume-hood, the air-dried latex was further dried in a vacuum oven at 70°C. The monomer conversion was calculated from the weight of monomers initially added and dried polymers obtained:

$$\text{Conversion (\%)} = \left(\frac{\text{Weight of dried latex} - \text{Weight of PEI and/or CS used}}{\text{Weight of monomer feed}}\right) \times 100,$$

$$\text{Solid content (\%)} = \left(\frac{\text{Weight of dried latex}}{\text{Weight of latex}}\right) \times 100.$$

2.2.3. Nanoparticle Characterization

The hydrodynamic diameter and polydispersity index (PDI) of nanoparticles were measured using a dynamic light scattering (DLS) method with a laser particle size analyzer (Malvern Instruments, UK) at 25°C. Then, the latex samples were dropped into the sample chamber with continuous stirring until the suitable concentration was attained, which was in the range of 1–5 wt%. The measurements were repeated three times. The surface charge of nanoparticles was measured by electrophoretic light scattering (ELS), using a zetasizer (NanoZS 4700, Malvern Instruments) in 1 mM NaCl solution at room temperature. The measurements were done at a wavelength of 633 nm at 25°C with a scattering angle of 90°. The results reported were the mean of three determinations. The morphology of nanoparticles was observed with scanning electron microscope (SEM, S-2500, Hitachi, Japan). To prepare the sample, 50 µl nanoparticle (10 mg/ml) dispersion was dropped on a cover glass and dried in a dust-free environment. The dried specimens were stuck on the sample

holders with a double-coated carbon conductive tab and then were sputter-coated under vacuum with platinum and palladium by using a sputter coater (E-102, Hitachi, Japan). The sputter-coated sample was observed by the microscope at 15 eV. Fourier-transform infrared (FT-IR) spectroscopy was used to confirm the grafting reaction of PMMA onto chitosan-PEI mixture. The dried nanoparticles were first extracted with dichloromethane for 2 days to separate the homo-PMMA to obtain the pure CS/PEI. FT-IR spectra of the samples were recorded in the attenuated total reflection mode using an FT-IR spectrophotometer (Equinox 55, Bruker) equipped with a single reflection ATR unit. The powder samples were pressed in contact between the internal reflection element (IRE) crystal and the gripper plate. The spectra were recorded at a resolution of 4 cm^{-1} and 32 scans. Each spectra scanning was done in the range between 4000 and 600 cm^{-1}. The weight fraction of PEI in the particles was obtained from the examination of FT-IR absorption intensity, by comparing the intensity of the signal at 1635 cm^{-1} (NH stretching from both CS and PEI) to that at 1546 cm^{-1} (NH complexed with acetic acid found in CS only). The standard calibration curve was first established by plotting the intensity ratio of the above the FT-IR signals and the weight fraction of PEI and CS dissolved in acetic acid.

2.2.4. Determination of the Buffering Capacity of Nanoparticles

The buffering ability of the nanoparticles was observed by recording the pH change during the titration of acidic nanoparticle dispersion with 0.1 M NaOH solution. Before titration, 2 ml of the nanoparticle (20 mg/ml) was dispersed in 15 ml of 150 mM NaCl solution, and then the pH of the dispersion was adjusted to 2 with 1.0 M HCl. The 0.1 M NaOH solution was added slowly to the dispersion, and the pH was recorded as function of the added NaOH solution.

2.2.5. Determination of Amine Groups at the Surface of Nanoparticles

The amount of amine groups on the nanoparticle surface was determined by the conventional 2,4,6-trinitrobenzene sulfonic acid (TNBS) assay. The nanoparticle dispersion was diluted to give a final concentration of 10 mg/ml and suspended in 100 µl of phosphate buffered saline solution (10 mM PBS, pH 7.6). Then, 200 µl of 4% $NaHCO_3$ solution (pH 8.5) and 200 µl of 1% TNBS aqueous solution were added. These mixtures were incubated at 37°C for 2 h. After incubation, 200 µl of the mixtures was added to each well of a 96-well culture plate and the absorbance of samples was measured at 415 nm using VERSAmax microplate reader (Molecular Devices, Sunnyvale, CA, USA). The amount of amine groups on the particle surface was calculated based on the calibration curve prepared by the β-alanine standard solution.

2.2.6. Preparation of Plasmid DNA

The plasmid DNA was pGL3 vector (5.26 kb), coding for a firefly luciferase gene (Luciferase Reporter Vectors-pGL3, Promega, Medison, WI, USA). The plasmid DNA was propagated in an *Escherichia coli* strain (DH5α) in 1 l LB medium supplemented with 100 µg/ml ampicillin at 37°C. The mixture was shaken overnight at

300 rpm. The amplified plasmid DNA was purified using the Qiagen Plasmid Mega and Giga kit (Qiagen, Tokyo, Japan) according to the manufacturers instructions. Both yield and purity of the plasmid DNA were evaluated by UV spectrophotometry (Ultrospec 2000, Pharmacia, Cambridge, UK) at wavelengths of 260 to 280 nm. The final concentration was adjusted to be 1 mg/ml.

2.2.7. Complex Formation of Plasmid DNA and CS/PEI Nanoparticles

The complexes were prepared by mixing an aqueous dispersion of nanoparticles with an aqueous solution of plasmid DNA. Briefty, various amounts of nanoparticles were suspended in 50 µl doubled-deionized water, mixed with 50 µl PBS containing 100 µg plasmid DNA, and left for 15 min at room temperature to obtain various complexes. The composition was calculated on the basic of the nitrogen number of nanoparticles (N) per the phosphorus number of plasmid DNA (P) and expressed as the N/P ratio. Nitrogen number of nanoparticles was determined using the TNBS method. The morphology of complexes was observed with SEM. To prepare the sample, 50 µl complex was dropped on a cover glass and dried in a dust-free environment. The dried specimens were stuck on the sample holders with a double-coated carbon conductive tab and then were sputter-coated under vacuum with platinum and palladium and observed under the microscope at 15 eV.

2.2.8. Gel Retardation Assay

Complexes were prepared in 10 mM PBS solution at different N/P ratios. After 15 min incubation, 7 µl of the complex was added to 3 µl loading buffer solution (0.1% sodium dodecyl sulfate, 5% glycerol and 0.005% bromophenol blue) and applied to a 1 wt% agarose gel in tris-borate-ethylenediaminetetraacetic acid buffer solution (TBE, pH 8.3) containing 0.1 mg/ml of ethidium bromide (EtBr). Electrophoretic evaluation was carried out in TBE solution at 100 V for 30 min. The gel was imaged with a UV transilluminator (Gel Doc 2000, Bio-Rad Laboratories, Segrate, Italy).

2.2.9. EtBr Intercalation Assay

A sample containing plasmid DNA (20 µg/ml) and EtBr (0.4 µg /ml) was used for standard calibration, which was set as 100% fluorescence intensity. MilliQ water and EtBr were used as a blank. The nanoparticle dispersion was added to an aqueous solution of EtBr at different N/P ratios. The fluorescence intensity was measured at excitation wavelength 510 nm and emission wavelength 590 nm by using the fluorescent microplate reader (Molecular Devices, Sunnyvale, CA, USA). The results were expressed as a relative fluorescence intensity (a percentage decrease of fluorescence intensity against the fluorescence intensity of the plasmid DNA–EtBr complex).

2.2.10. Cell Culture

MSCs were isolated from bone shaft of femurs of 3-week-old male Wistar rats. Both ends of rat femurs were cut away from the epiphysis, and the bone marrow was flushed out with a syringe (21-gauge needle) with 1 ml minimal essential al-

pha medium (αMEM) supplemented with 10% fetal bovine serum (FBS). The cell suspension (5 ml) was placed into two T-25 flasks (Iwaki Glass, Funabashi, Chiba, Japan) at 37°C under 5% CO_2. The medium was replaced on the fourth day of culture and every three days thereafter. When the cells of the first passage became sub-confluent, usually within 7–10 days after seeding, the cells were detached from the flask by treatment with a solution of 0.25 wt% trypsin and 0.02 wt% ethylenediaminetetraacetic acid (EDTA) in PBS for 5 min at 37°C. The cells of second-passage were used for next experimental steps.

2.2.11. In Vitro *Gene Transfection Experiment*

Transfection experiments were performed independently in triplicate. In a 6-well plate (Corning, NY, USA), MSCs were seeded at a density of 5×10^4 cells/well and cultured in 2 ml αMEM-FBS for 24 h. The complexes were formed by mixing 50 µl nanoparticle dispersion in MilliQ water and 50 µl PBS containing 5 µg of pGL-3-luciferase plasmid DNA at different N/P ratios, followed by incubation for 15 min at room temperature. Immediately after the medium was replaced with fresh Opti αMEM medium, 100 µl of the complex solution was added and followed by a 6-h incubation for cell transfection. Then, the medium was changed to αMEM-FBS and cells were incubated further for 24 h. As a positive control, the cells were treated with the complexes of 250 µl MilliQ water containing 10 µg Lipofectamine™ 2000 (Invitrogen) and 250 µl PBS containing 4 µg pGL-3-luciferase plasmid DNA. Untreated cells were assigned as negative control. Then the cells were washed with PBS and lysed with 200 µl of cell-culture lysis reagent (Promega, Madison, WI, USA). The cell debris was separated by centrifugation (at 14×10^3 rpm, 20 min). Then, 100 µl luciferase assay reagent (Promega) was added to 20 µl supernatant. The relative light unit (RLU) of the samples was determined by a luminometer (MicroLumatPlus LB 96V, Berthold, Tokyo, Japan). The experiments were preformed in triplicate. The total protein content in each well was determined using the bicinchonic acid (BCA) protein assay kit (Pierce, Rockford, IL, USA), according to the manufacturer instruction in order to normalize the influence of number variance of cells on the luciferase activity. The gene expression profile at various post-transfection times (1, 3, 5 and 7 days) was determined. The transfected cells were cultured in αMEM-FBS at 37°C under 5% CO_2. The medium was replaced every three days thereafter.

2.2.12. Cell Viability

Cytotoxicity was assayed using a cell counting kit (Nacalai Tesque, Kyoto, Japan). The cells were seeded at 5×10^4 cells per well in a 96-well plate using αMEM-FBS, and incubated at 37°C for 24 h under a 5% CO_2 atmosphere. The medium was replaced with Opti αMEM medium, and 10 µl of the complex dispersion was added to each well and subsequently incubated with the cells for 6 h. The medium was then replaced with 100 µl fresh αMEM-FBS and 10 µl 2-(2-methoxy-4-nitrophenyl)-3-(4-nitrophenyl)-5-(2,4-disulfophenyl)-2H-tetrazolium (WST-8) solution. The samples were further incubated at 37°C for 3 h. The absorbance of samples was mea-

sured at 450 nm using a VERSAmax microplate reader (Molecular Devices). The cell viability (%) was calculated according to the following equation:

$$\text{Cell viability (\%)} = (A_{\text{sample}}/A_{\text{control}}) \times 100, \quad (1)$$

where A_{sample} is the absorbance of the complex and A_{control} is the absorbance of the untreated cells. The results reported were the mean of eight determinations.

2.2.13. Statistical Analysis

All the data were expressed as the mean ± the standard deviation of the mean. Statistical analysis was performed based on the ANOVA, followed by Fisher's PLSD and the significance was accepted at $P < 0.05$.

3. Results

3.1. Preparation of Nanoparticles

Nanoparticles with a PMMA core and PEI and/or CS shell were prepared by the emulsifier-free emulsion polymerization. Table 1 summarizes the monomer conversions and solid contents of the nanoparticles after polymerization. It can be observed that the monomer conversions increased with the amount of PEI added to CS, from 75 to 96%, and the monomer conversion in case of PEI alone was about 79%. The solid contents of the latexes were in the range of 2.49–4.42%.

3.2. Characterization of Nanoparticles

Table 2 shows the sizes of nanoparticles as determined by the DLS and SEM analyses. PEI nanoparticles had a diameter around 216 nm when measured by the DSL, but 314 nm from SEM. In the CS/PEI systems, the nanoparticle diameters were in the range of 129–162 nm (from DSL) and 182–224 nm (from SEM), depending on the amount of PEI incorporated. The polydispersity index (PDI) of CS nanoparticles was 1.3, while the PDI values of the CS/PEI and PEI nanoparticles were lower, ranging from 1.17 to 1.25. The surface charges of all nanoparticles were obtained from zeta-potential measurement (Table 2). The surface charge at pH 7 was found to

Table 1.
Preparation of CS, CS/PEI and PEI nanoparticles with different amounts of PEI introduced

Sample	CS/PEI (w/w)	Conversion (%)[a]	Solid content (%)
CS	0.5:0	74.6 ± 2.6	2.40 ± 0.05
CS/PEI 1	0.5:0.1	78.2 ± 2.8	2.87 ± 0.06
CS/PEI 3	0.5:0.3	90.6 ± 5.7	3.72 ± 0.11
CS/PEI 5	0.5:0.5	95.8 ± 7.6	4.42 ± 0.15
PEI	0:0.5	79.3 ± 2.5	3.09 ± 0.05

[a] Polymerization at 80°C under N_2 atmosphere for 2 h.

Table 2.
Particle size obtained by DLS and SEM analysis and zeta potential of CS, PEI and CS/PEI nanoparticles with different amounts of PEI introduced

Nanoparticle	DLS (nm)	SEM (nm)	Polydispersity[a]	Zeta potential (mV)[b]
CS	162 ± 6.9	182 ± 20	1.30	-3.0 ± 0.2
CS/PEI 1	156 ± 23.7	224 ± 21	1.25	$+22.0 \pm 0.1$
CS/PEI 3	144 ± 19.6	194 ± 20	1.26	$+24.0 \pm 0.3$
CS/PEI 5	129 ± 10	189 ± 20	1.17	$+30.5 \pm 0.2$
PEI	216 ± 39.8	314 ± 24	1.18	$+36.8 \pm 0.1$

[a] Polydispersity index $= D_v/D_s$, where D_v is the volume average diameter and D_s the surface average diameter.
[b] Determined at pH 7 in 1 mM NaCl solution at room temperature.

increase dramatically from a negative value of CS nanoparticle to positive with PEI introduction. The PEI nanoparticles exhibited the highest zeta potential at +37 mV.

Figure 2 shows the SEM photographs of nanoparticles. It is apparent that all the nanoparticles possessed a spherical shape with uniform size distribution. For CS nanoparticles, the aggregation of nanoparticles was observed. However, when PEI was added into the system (CS/PEI), the extent of nanoparticle aggregation was decreased.

Figure 3 shows the FT-IR spectra of grafted products compared to those of chitosan and PEI. The spectrum of 85% deacetylated chitosan (Fig. 3a), showing a broad peak at 3500–3200 cm^{-1}, was attributed to an O–H stretching (3439 cm^{-1}) and N–H stretching (3365 cm^{-1}). The peak at 2892 cm^{-1} corresponded to C–H stretching vibrations. The characteristic peaks observed at 1649 cm^{-1} and 1599 cm^{-1} indicated the amide I (C=O stretching) and amide II (N–H bending), respectively, due to the remaining acetamide groups in chitosan. However, in the presence of acetic acid, CS exhibited the two major peaks at 1630 cm^{-1} ($-NH_3^+$ asymmetric deformation) and 1546 cm^{-1} ($-NH_3^+$ complexed with $-COO^-$). The spectrum of 50 wt% PEI showed the characteristic peaks at 3500–3200 cm^{-1} (O–H stretching and N–H stretching), 2949 cm^{-1} (asymmetric stretching of $-CH_2$), 2847 cm^{-1} (symmetric stretching of CH_2) and 1610 cm^{-1} ($-NH_3^+$ and $-NH_2^+$ deformation). For the grafted products, their spectra were similar to chitosan and PEI. Moreover, the additional signal was observed at 1730 cm^{-1}, which corresponded to the C=O stretching, and indicated the presence of grafted PMMA. However, the signal of C=O stretching decreased when the amount of PEI increased. This may be due to the fact that upon increasing the amount of PEI, the shell thickness of resulted nanoparticles would be increased. This could limit the penetration of the incident beam on the reflection mode of the FT-IR to the inner layer of the nanoparticles. Therefore, the C=O signal belonging to the grafted PMMA located at the inner part appeared with the lower intensity when the amount of PEI was increased.

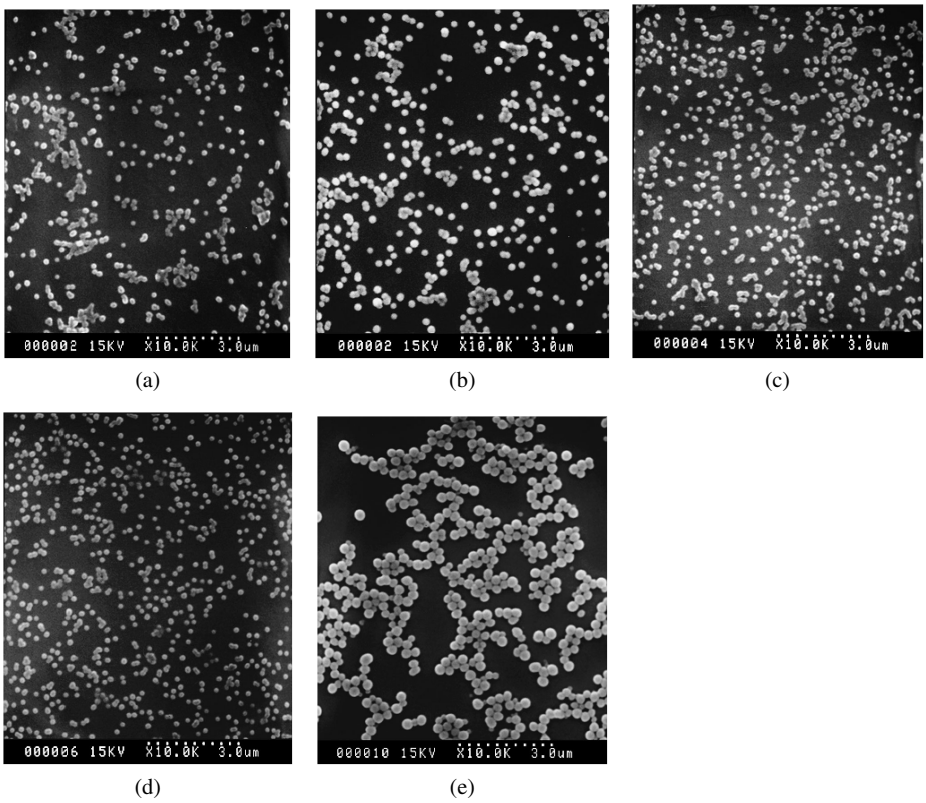

Figure 2. SEM images of nanoparticles. (a) CS, (b) CS/PEI 1, (c) CS/PEI 3, (d) CS/PEI 5 and (e) PEI at the same magnification.

The weight fraction of PEI introduced to the mixed systems analyzed from the FT-IR absorption intensity is shown in Table 3. By comparing the intensity of peaks around 1635 cm^{-1} (found from both PEI and chitosan) and at 1546 cm^{-1} (found in CS only) with the standard calibration curve, the weight fractions of PEI on the particles were calculated to be 0.45–0.51.

3.3. Determination of Amine Groups at the Nanoparticle Surface Using the TNBS Assay

Based on the TNBS assay, the amount of free amine groups on the nanoparticle surfaces can be derived to be 9.43, 19.05, 39.60, 56.75 and 38.06 μmol/ml for CS, CS/PEI 1, CS/PEI 3, CS/PEI 5 and PEI, respectively.

3.4. Buffering Capacity

Figure 4 shows the change of pH upon titration. For the CS nanoparticles, a rapid change was observed. The solution pH of CS/PEI nanoparticles changed more slowly. The higher the amount of PEI introduced, the slower the change of pH values.

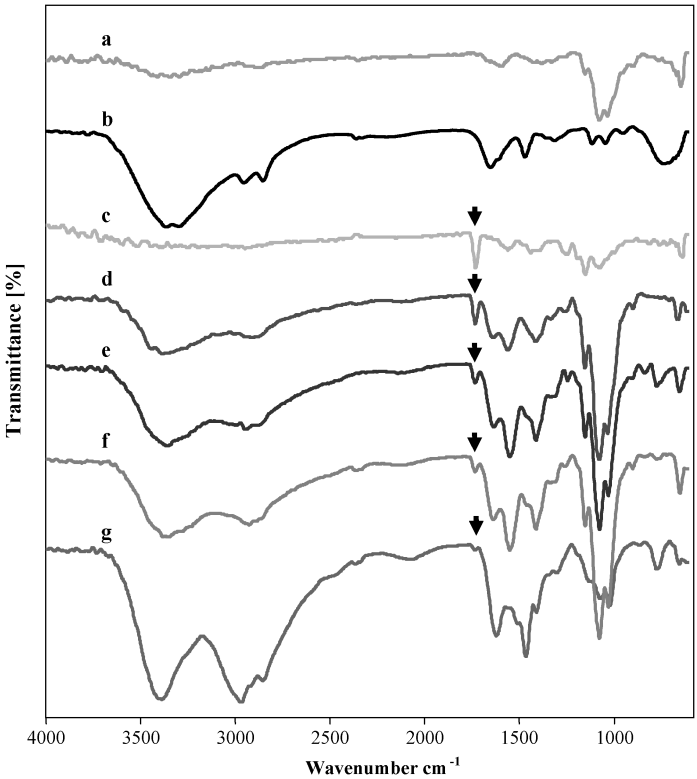

Figure 3. FT-IR spectra of prepared nanoparticles after Soxhlet extraction. (a) CS powders, (b) PEI polymer, (c) CS nanoparticles, (d) CS/PEI 1 nanoparticles, (e) CS/PEI 3 nanoparticles, (f) CS/PEI 5 nanoparticles and (g) PEI nanoparticles.

Table 3.
Weight ratios of PEI to CS introduced to nanoparticles obtained by FT-IR analysis

Nanoparticle (nm)	Weight fraction of PEI	
	In feed	In nanoparticles
CS/PEI 1	0.17	0.51
CS/PEI 3	0.38	0.47
CS/PEI 5	0.50	0.45

3.5. Characterization of Nanoparticles–Plasmid DNA Complexes

Figure 5 shows the electrophoretic patterns of nanoparticles–plasmid DNA complexes at different N/P ratios. Migration of plasmid DNA was retarded with an increase in the N/P ratio. No migration was seen at N/P ratios higher than 0.5. It is

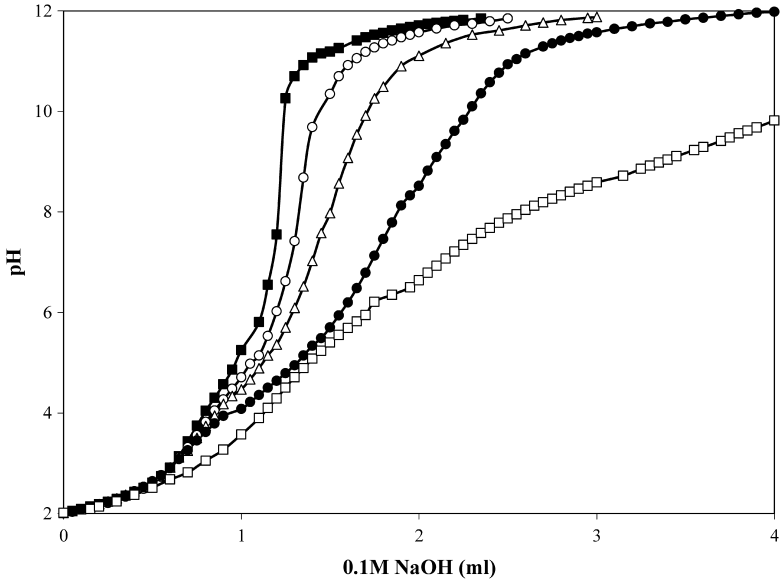

Figure 4. Titration curves obtained by titrating aqueous solutions of CS (■), CS/PEI 1 (○), CS/PEI 3 (△), CS/PEI 5 (●) and PEI (□) nanoparticles in 150 mM aqueous NaCl with 0.1 M NaOH.

apparent from the electrophoresis analysis that the plasmid DNA complexes were formed at the N/P ratio of 0.5 or higher, irrespective of the nanoparticle type.

Figure 6 shows the nanoparticle–plasmid DNA interaction evaluated by EtBr intercalation assay. This relative fluorescence of plasmid DNA intercalation with EtBr was reduced by the addition of nanoparticles as competing components to EtBr for plasmid DNA binding. It can be seen that the relative fluorescence intensities for all complexes were lowest at N/P ratios over 0.5.

Table 4 shows the particle size of nanoparticles–plasmid DNA complexes at N/P = 1.0. The reduction of particle sizes was due to the negatively charged pDNA partially neutralizing the positively charged chitosan shell.

3.6. Transfection Activity

Figure 7 shows the effect of various nanoparticles on the level of gene expression for MSC. The level of expression depended on the type of nanoparticle used for complexation. For every type of nanoparticle, the highest level was observed at the N/P ratio of 1.0. The level of expression decreased in the order CS/PEI 5, PEI, CS/PEI 3, CS/PEI 1, Lipofectamine and CS, respectively.

Figure 8 shows that the expression level for the case of Lipofectamine and PEI nanoparticles decreased rapidly. In contrast, the CS/PEI nanoparticles–plasmid DNA complexes exhibited gene expression for longer time periods.

3.7. Cytotoxicity Study

Figure 9 shows the viability of MSC 6 h after incubation with the complexes. At a N/P ratio of 1, where the highest transfection was observed, the cell viability de-

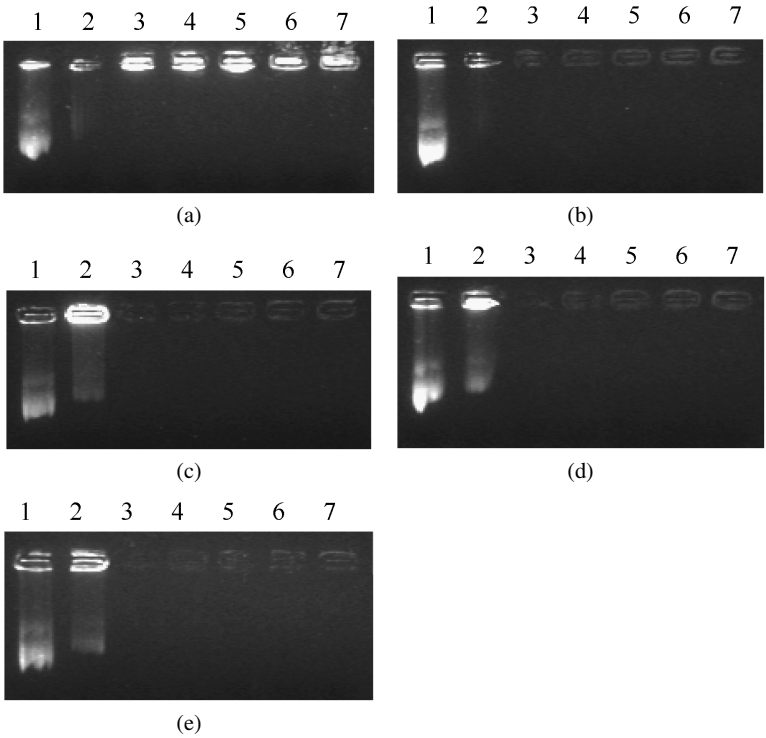

Figure 5. N/P ratios of nanoparticles to plasmid DNA required for complete complexation. (a) CS, (b) CS/PEI 1, (c) CS/PEI 3, (d) CS/PEI 5 and (e) PEI. Lanes: 1, DNA marker; 2–7, particles/pDNA at N/P ratios of 0.1, 0.5, 1.0, 1.5, 3.0 and 5.0, respectively.

creased significantly for the PEI nanoparticles, while that of the CS/PEI 1, CS/PEI 3 and CS/PEI 5 did not. The CS/PEI nanoparticles showed lower cytotoxicity compared with the PEI nanoparticles at the corresponding N/P ratio.

4. Discussion

As described in the Materials and methods section, PEI and CS have free amine groups capable of forming redox pairs with TBHP to generate free radicals on amine N atoms of PEI and CS. Once the TBHP and NH_2 groups of CS and PEI form a redox pair, the graft co-polymerization of MMA onto CS–PEI is initiated. These grafted copolymers consisting of hydrophilic CS/PEI and the hydrophobic PMMA chains, which then spontaneously formed nanoparticles in an aqueous medium. It is conceivable from the viewpoint of thermodynamics that the hydrophobic segment is condensed to the central core of nanoparticles, and the hydrophilic segment is enwrapped the hydrophobic core, resulting in core–shell nanoparticles. These nanoparticles are stabilized by the positive charges of the CS/PEI shell layer.

The increase of monomer conversion with the amount of PEI introduced is due to the increasing amount of amine groups. Since the amine groups can form redox

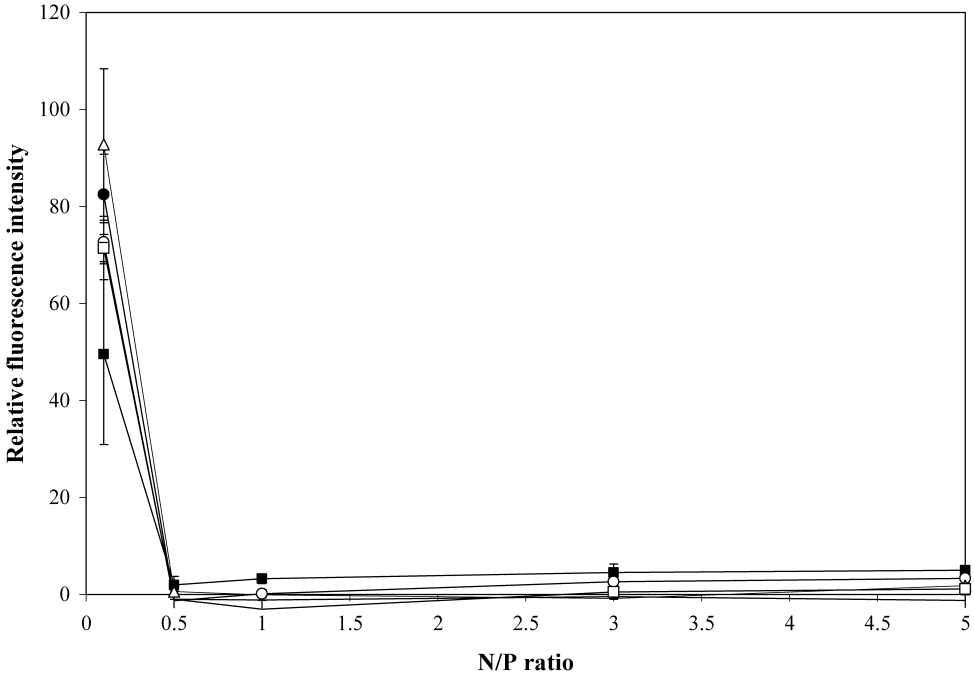

Figure 6. Relative fluorescence intensity of CS (■), CS/PEI 1 (○), CS/PEI 3 (△), CS/PEI 5 (●) and PEI (□) nanoparticles at different N/P ratios intercalated with EtBr. A sample containing plasmid DNA (20 μg/ml) and EtBr (0.4 μg/ml) was used for standard calibration, which was set as 100% fluorescence intensity. MilliQ water and EtBr were used as a blank. The fluorescence intensity was measured at excitation wavelength 510 nm and emission wavelength 590 nm.

Table 4.
Particle size of original nanoparticles and nanoparticles-plasmid DNA complexes at N/P = 1.0 obtained by SEM analysis

Nanoparticle	Size (nm)	
	Before DNA complexation	After DNA complexation
CS	182 ± 20	180 ± 19
CS/PEI 1	224 ± 21	197 ± 22
CS/PEI 3	194 ± 20	186 ± 25
CS/PEI 5	189 ± 20	177 ± 19
PEI	314 ± 24	289 ± 28

pairs with TBHP, with an increase in the amine groups, it is likely that more redox pairs are formed to generate free radicals. This could accelerate the polymeriza-

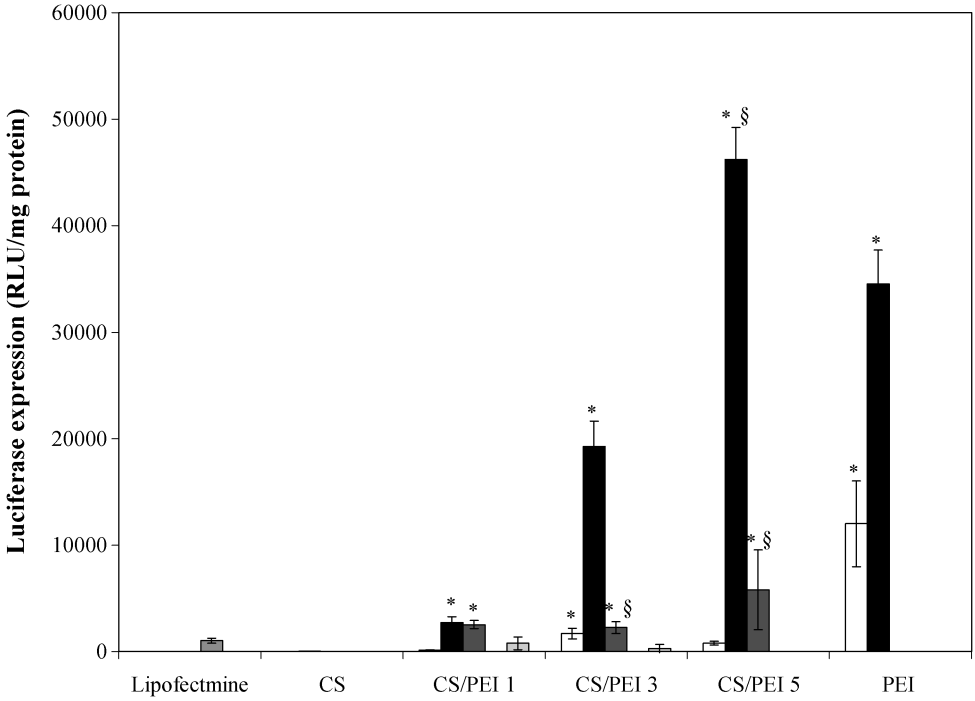

Figure 7. *In vitro* luciferase transfection expression of Lipofectamine, CS CS/PEI 1, CS/PEI 3, CS/PEI 5 and PEI at different N/P ratios: 0.5 (□), 1 (■), 3 (■), 4 (■) and 5 (□) after day 1 post-transfection. $^{*}P < 0.05$, significant against the expression level of Lipofectamine; $^{\S}P < 0.05$, significant against the expression level of PEI at the corresponding ratio.

tion and result in higher monomer conversion. The solid contents depended on the amount of CS and PEI introduced, and the monomer conversion percentage.

The introduction of polyethyleneimine to chitosan before emulsion polymerization can affect the size of resulted nanoparticles as shown in Table 2. The size of CS/PEI nanoparticles tended to decrease with the increasing amount of PEI introduced. Since the mechanism in this polymerization system was initiated by free radicals generated from amine and TBHP. It is possible that the PEI introduction increased the amine content, resulting in more initiating radicals for polymerization. Then the surfactant-like species, which involved in the particle stabilization, were also increased, resulting in the smaller particle size [24].

The narrow size distribution of nanoparticles would come from the effective nucleation and growth of the nanoparticles in this system. In addition, their presence on the surface will enable nanoparticles to enhance electrostatic stabilization, which prevent the growing nanoparticles from aggregation. It can be observed from the SEM images (Fig. 2) that PEI incorporation gave the nanoparticles a uniform size distribution.

The increase in the amount of PEI contributes to an increase of amine groups on the nanoparticle surface. The number of amine groups further increased by the

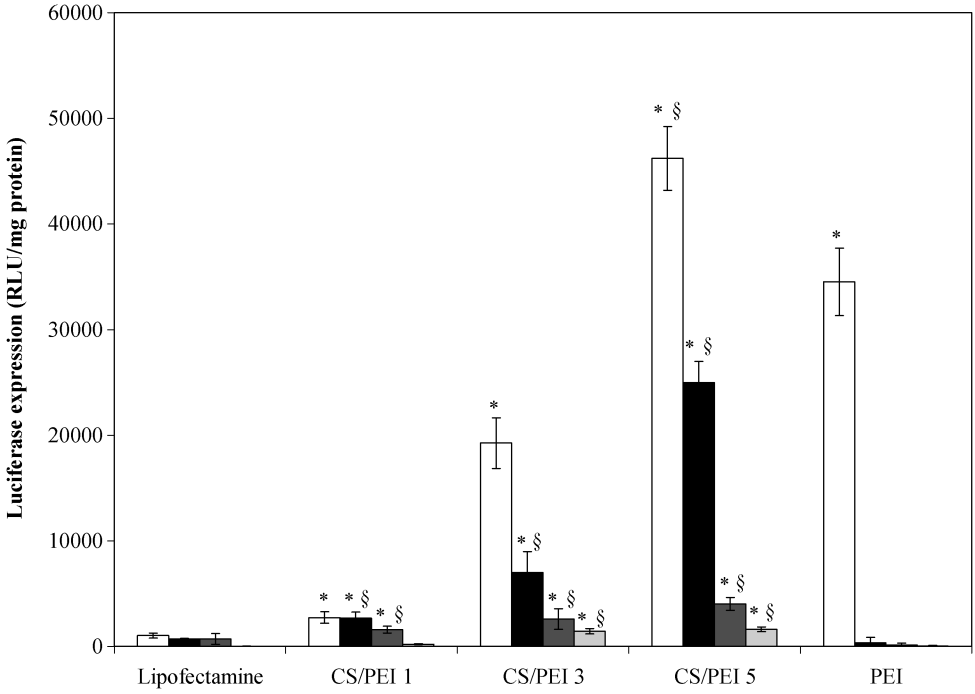

Figure 8. *In vitro* transfection profile of Lipofectamine, PEI, CS/PEI 1, CS/PEI 3 and CS/PEI 5 after days 1 (□), 3 (■), 5 (■) and 7 (□) post-transfection. $^{*}P < 0.05$, significant against the expression level of Lipofectamine; $^{\S}P < 0.05$, significant against the expression level of PEI at the corresponding post-transfection.

addition of PEI on the nanoparticle surfaces. In acidic conditions, the nanoparticle surface is of positive charge because the amine groups of PEI and chitosan on the nanoparticle surface are protonated. The surface charge would enable the nanoparticles to homogeneously disperse in the aqueous medium through an electrostatic repulsion force. The positive character contributed to the high capability to complex electrostatically with negatively charged plasmid DNA.

It is known that the buffering effect of PEI facilitates endosomal escape [18]. In this study, this property was observed in the PEI-incorporated nanoparticles as well. In Fig. 4, the buffering effect of PEI nanoparticles is demonstated by a slow change of pH of solution. In contrast, the solution pH of CS nanoparticles showed a rapid change. Upon increasing the amount of PEI in the CS/PEI systems, the change was retarded. This retardation of pH change would mainly be due to the buffering effect of PEI, and this effect can be observed even in the form of nanoparticles. In addition, the buffering effect of nanoparticles was found to be affected by the PEI incorporation. This clearly indicates that PEI present in the surface of CS/PEI nanoparticles can maintain its buffering ability.

Electrophoretic results indicated that the nanoparticles could form a complex with the plasmid DNA at N/P ratios of 0.5 or higher, which corresponded well to

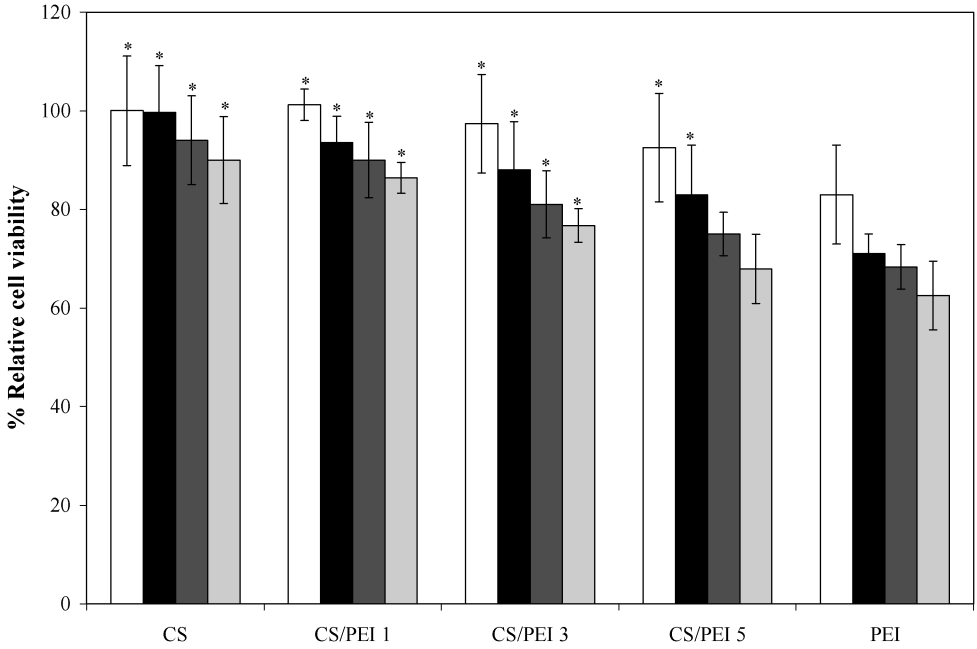

Figure 9. The cell viability of rMSCs transfected with CS/PEI nanoparticle–plasmid DNA complexes prepared at different N/P ratios: 0.5 (□), 1 (■), 3 (■) and 5 (□). * $P < 0.05$, significant against the relative cell viability of PEI at the corresponding ratio.

the result of the EtBr intercalation assay. When comparing the retardation rate between various nanoparticles prepared at N/P ratios of 0.5–1.0, the CS nanoparticles showed the lowest rate, while the PEI and CS/PEI showed a similar profile. It is likely that the PEI and CS/PEI nanopartcles rapidly formed a complex with the plasmid DNA because the large number of positive amine groups on the surface causes stronger electrostatic interaction with the plasmid DNA, as evidenced by the reduction of complex size.

In general, PEI has been revealed to be a most effective non-viral vector due to its high pH buffering capacity, providing high concentration of protanable amine and imine groups, which are believed to enhance the release of carriers from the endosomal compartment [18, 21]. However, PEI has a major drawback on its toxicity that can limit the application in gene therapy. In contrast, the low transfection efficiency of chitosan was agreed with several works [20, 22, 25]. This limitation was caused by the inefficient endosomal escape [25]. It has been reported that the ability for complexes to escape the endosomal compartment can be correlated to the buffering capacity of the polymer [26, 27]. Therefore, in order to improve the transfection efficiency, modification of chitosan is of great consideration.

In this study, the combination of high transfection ability of PEI and biocompatibility of CS was attempted. The gene transfection for a superior transfection efficiency was observed compared with commercially available Lipofectamine, as

expected. The *in vitro* gene expression of plasmid DNA was greatly enhanced by the introduction of PEI to CS nanoparticles. Also, the amount of PEI incorporated showed significant influence. This high efficiency of CS/PEI may be due to the presence of PEI. The PEI has enhanced buffering capacity in the endosomal compartment of cells. The rapid gene expression induction of PEI attributed to a fast endosomal escape, which was correlated with the results of Artursson and co-workers [19]. Its high efficiency may also be due to the enhancement of gene transportation from the cytoplasm to the nucleus. In addition, the highest expression for CS/PEI 5 might be due to the lower toxicity of CS/PEI 5 comparing with PEI itself.

It can be seen from the results that CS/PEI nanoparticles showed the high transfection efficiency and prolonged gene expression. It was hypothesized that the CS/PEI nanoparticles have less toxicity as indicated by the high percentage of cell viability. A more detailed investigation is under way.

It is also known that the cause of PEI cytotoxicity may be due to the multiple attachment of PEI to the cell surface, resulting in lysis of the cell [28]. In case of the CS/PEI, although PEI was combined in the particles, the cell viability was still high at the corresponding N/P ratio. However, the decrease in relative cell viability was related with the amount of PEI incorporated as well as the increase of N/P ratio. The existence of CS could lower the cytotoxicity of the particles, if the PEI content is low. In addition, it is possible that this low cytotoxicity gives rise to enhanced gene transfection and prolonged expression.

5. Conclusion

PEI-introduced CS nanoparticles showed promising particle size, dispersity, surface charge and buffering capacity, from the viewpoint of gene transfection carrier. Gene transfection of CS/PEI nanoparticles for MSCs was achieved with an efficiency higher than that of chitosan and Lipofectamine. It is possible that the increase in amine groups from PEI leads to the enhanced buffering ability in the endosomal compartment. CS/PEI 5 exhibited a higher transfection ability than the original PEI and, additionally, lower toxicity. It can be concluded that the combination of chitosan and PEI on the nanoparticles is promising as gene-delivery carriers for MSCs.

Acknowledgements

This research was financially supported by the National Nanotechnology Center, Thailand (Project code NN-B-22-m37-94-49-54), Thailand Graduate Institute of Science and Technology (TGIST) and the Insitute for Frontier Medical Science, Kyoto University, Japan. We would like to acknowledge with thanks Mr. Jun-ichiro Jo for his comments and assistance with MSCs isolation.

References

1. M. Krampera, G. Pizzolo, G. Aprili and M. Franchini, *Bone* **39**, 678 (2006).
2. M. F. Pittenger, A. M. Mackay, S. C. Beck, R. K. Jaiswal, R. Douglas, J. D. Mosca, M. A. Moorman, D. W. Simonetti, S. Craig and D. R. Marshak, *Science* **284**, 143 (1999).
3. D. J. Prockop, *Science* **276**, 71 (1997).
4. T. Y. Hui, K. M. C. Cheung, W. L. Cheung, D. Chan and B. P. Chan, *Biomaterials* **29**, 3201 (2008).
5. J. M. Kanczler, P. J. Ginty, J. J. A. Barry, N. M. P. Clarke, S. M. Howdle, K. M. Shakesheff and R. O. C. Oreffo, *Biomaterials* **29**, 1892 (2008).
6. W. Ando, K. Tateishi, D. A. Hart, D. Katakai, Y. Tanaka, K. Nakata, J. Hashimoto, H. Fujie, K. Shino, H. Yoshikawa and N. Nakamura, *Biomaterials* **28**, 5462 (2007).
7. B. P. Chan, T. Y. Hui, C. W. Yeung, J. Li, I. Mo and G. C. F. Chan, *Biomaterials* **28**, 4652 (2007).
8. C. Kirker-Head, V. Karageorgiou, S. Hofmann, R. Fajardo, O. Betz, H. P. Merkle, M. Hilbe, B. von Rechenberg, J. McCool, L. Abrahamsen, A. Nazarian, E. Cory, M. Curtis, D. Kaplan and L. Meinel, *Bone* **41**, 247 (2007).
9. H. Park, J. S. Temenoff, Y. Tabata, A. I. Caplan and A. G. Mikos, *Biomaterials* **28**, 321 (2007).
10. D. S. W. Benoit, C. R. Nuttelman, S. D. Collins and K. S. Anseth, *Biomaterials* **27**, 6102 (2006).
11. Y. Takahashi, M. Yamamoto and Y. Tabata, *Biomaterials* **26**, 3587 (2005).
12. L. Meinel, S. Hofmann, O. Betz, R. Fajardo, H. P. Merkle, R. Langer, C. H. Evans, G. Vunjak-Novakovic and D. L. Kaplan, *Biomaterials* **27**, 4993 (2006).
13. H. H. Ahn, J. H. Lee, K. S. Kim, J. Y Lee, M. S. Kim, G. Khang, I. W. Lee and H. B. Lee, *Biomaterials* **29**, 2415 (2008).
14. B. A. Clements, V. Incani, C. Kucharski, A. Lavasanifar, B. Ritchie and H. Uludag, *Biomaterials* **28**, 4693 (2007).
15. H. Hosseinkhani, T. Azzam, H. Kobayashi, Y. Hiraoka, H. Shimokawa, A. J. Domb and Y. Tabata, *Biomaterials* **27**, 4269 (2006).
16. J.-I. Jo, N. Nagaya, Y. Miyahara, M. Kataoka, M. Harada-shida, K. Kangawa and Y. Tabata, *Tissue Eng.* **13**, 313 (2007).
17. D. Schaffert and E. Wagner, *Gene Ther.* **15**, 1131 (2008).
18. W. T. Godbey, K. K. Wu and A. G. Mikos, *J. Control. Rel.* **60**, 149 (1999).
19. M. Koping-Hoggard, K. M. Varum, M. Issa, S. Danielsen, B. E. Christensen, B. T. Stokke and P. Artursson, *Gene Ther.* **11**, 1441 (2004).
20. K. Roy, H.-Q. Mao, S.-K. Huang and K. W. Leong, *Nature Med.* **5**, 387 (1999).
21. M. Koping-Hoggard, I. Tubulekas, H. Guan, K. Edwards, M. Nilsson, K. M. Varum and P. Artursson, *Gene Ther.* **8**, 1108 (2001).
22. F. C. MacLaughlin, R. J. Mumper, J. Wang, J. M. Tagliaferri, I. Gill, M. Hinchcliffe and A. P. Rolland, *J. Control. Rel.* **56**, 259 (1998).
23. N. Pimpha, U. Rattanonchai, S. Surassmo, P. Opanasopit, C. Rattanarungchai and P. Sunintaboon, *Colloid Polym. Sci.* **286**, 907 (2008).
24. J. Xu, P. Lei and C. Wu, *J. Polym. Sci.: Part A: Polym. Chem.* **37**, 2069 (1999).
25. H.-Q. Mao, K. Roy, V. L. Troung-Le, K. A. Janes, K. Y. Lin, Y. Wang, J. T. August and K. W. Leong, *J. Control. Rel.* **70**, 399 (2001).
26. M. X. Tang and F. C. Szoka, *Gene Ther.* **4**, 823 (1997).
27. R. Wattiaux, N. Laurent, S. W.-D. Coninck and M. Jadot, *Adv. Drug Deliv. Rev.* **41**, 201 (2000).
28. D. Fischer, Y. Li, B. Ahlemeyer, J. Krieglstein and T. Kissel, *Biomaterials* **24**, 1121 (2003).

Copyright of Journal of Biomaterials Science -- Polymer Edition is the property of VSP International Science Publishers and its content may not be copied or emailed to multiple sites or posted to a listserv without the copyright holder's express written permission. However, users may print, download, or email articles for individual use.